



Application of the Polar WRF model for Svalbard — sensitivity to planetary boundary layer, radiation and microphysics schemes

Natalia PILGUJ*¹, Bartosz CZERNECKI², Maciej KRYZA¹,
Krzysztof MIGAŁA¹ and Leszek KOLENDOWICZ²

¹ *Department of Climatology and Atmosphere Protection, Institute of Geography
and Regional Development, University of Wrocław,
Aleksandra Kosiby 8, 51-621 Wrocław, Poland*

² *Department of Climatology, Institute of Physical Geography and Environmental Planning,
Adam Mickiewicz University, in Poznań
Bogumiła Krygowskiego 10, 61-680 Poznań, Poland*

* *corresponding author <natalia.pilguj@uwr.edu.pl>*

Abstract: This paper constitutes the sensitivity study of application the Polar WRF model to the Svalbard area with testing selected parameterizations, including planetary boundary layer, radiation and microphysics schemes. The model was configured, using three one-way nested domains with 27 km, 9 km and 3 km grid cell resolutions. Results from the innermost domain were presented and compared against measured wind speed and air temperature at 10 meteorological stations. The study period covers two months: June 2008 and January 2009. Significant differences between simulations results occurred for planetary boundary layer (PBL) schemes in January 2009. The Mellor-Yamada-Janjic (MYJ) planetary boundary layer (PBL) scheme resulted in the lowest errors for air temperature, according to mean error (ME), mean absolute error (MAE) and correlation coefficient values, where for wind speed this scheme was the worst from all the PBL schemes tested. In the case of June 2008, shortwave and longwave radiation schemes influenced the results the most. Generally, higher correlations were obtained for January, both for air temperature and wind speed. However, the model performs better for June in terms of ME and MAE error statistics. The results were also analyzed spatially, to summarize the uncertainty of the model results related to the analyzed parameterization schemes groups. Significant variability among simulations was calculated for January 2009 over the northern part of Spitsbergen and fjords for the PBL schemes. Standard deviations for monthly average simulated values were up to 3.5°C for air temperature and around 1 m s⁻¹ for wind speed.

Key words: Arctic, dynamical downscaling, parameterizations testing, numerical modeling, model evaluation.

Introduction

Polar regions are covered with sparse meteorological measuring network. On the other hand, these areas are very sensitive to climate changes. For example, Svalbard is a region covered with large number of research that look for the links between climate, climate change and ecosystems (Hodkinson *et al.* 1998; Stempniewicz *et al.* 2007; Wassmann *et al.* 2011), glacier melting (Radić *et al.* 2014), sea ice extent (Rothrock *et al.* 1999; Stroeve *et al.* 2007) or air pollution (Law and Stohl 2007). For these studies, it is necessary to have access to high resolution meteorological information, especially considering the complexity of the terrain and land-sea interactions. One source of such data is dynamic downscaling of global gridded meteorological data, with regional meteorological models working at higher spatial resolutions (Hong and Kanamitsu 2014). High-resolution models benefit from detailed surface information such as land use or orography, and therefore allows to represent local features, like sea breeze or katabatic winds (Heikkilä *et al.* 2011; Czernecki and Pótrolniczak 2013). Mesoscale numerical weather prediction (NWP) models, such as Weather Research and Forecasting (WRF; Skamarock *et al.* 2005) and its modification for the polar areas — Polar WRF — are the examples of the tools that are used for dynamical downscaling at high spatial and temporal resolution. The Polar WRF model has been successfully tested for Greenland ice sheet (Hines and Bromwich 2008), Arctic Ocean (Bromwich *et al.* 2009), western Arctic (Hines *et al.* 2011) and Antarctica (Kumar *et al.* 2012; Bromwich *et al.* 2013). In addition, the standard version of the WRF model has been often applied for polar area research (Mäkiranta *et al.* 2011; Tastula and Vihma 2011). In some studies, focused on *e.g.* vertical structure of boundary layer or variability of meteorological elements, the differences between WRF and Polar WRF were found marginal (Tastula and Vihma 2011; Kilpeläinen *et al.* 2012). Modifications of Polar WRF refers mainly to the treatment of fractional sea ice and its frequency within grid scale, so this model may outperform standard WRF over the sea ice zone (Tastula and Vihma 2011).

The above mentioned studies were undertaken with the WRF or Polar WRF models, but usually with different configurations in terms of domain settings (including spatial and vertical resolution), or physics. The increasing computational power allows for application of the NWP at high spatial resolution over the large areas, and studies from various areas show the added value of increased spatial resolution (Kotlarski *et al.* 2014). This is of special significance for the areas like Svalbard, where complex topography of the coasts (fjords and mountain ranges) further strongly affects the atmospheric processes and spatial distribution of meteorological variables (Kilpeläinen *et al.* 2011; Vihma *et al.* 2014). However, the relation between the horizontal resolution of the model domain and model performance is not always very straightforward, as was

shown by the Claremar *et al.* (2012). Claremar *et al.* (2012) have also shown that the different parameterizations of *e.g.* atmospheric boundary layer, have limited impact on the model performance. The role of model parameterization is also highlighted by Giorgi and Gutowski (2015).

Many papers include high resolution simulations for parts of Svalbard area, mostly fjords (*e.g.* Kilpeläinen *et al.* 2011; Láska *et al.* 2017). In this work, we have applied the polar WRF model at high spatial resolution for the entire area of Svalbard. The model has been run for different schemes of planetary boundary layer, microphysics and short- and longwave radiation, and we analyzed the model sensitivity for these parameterizations. The performance of the model for each scheme has been quantified for air temperature and wind speed using the available meteorological measurements for two different months, with June 2008 and January 2009 as examples. Furthermore, we investigate how these schemes influence the model results spatially, by calculating mean and standard deviations gridded information from all the model runs.

Materials and methods

Model configuration and parameterization schemes. — In this study, the Polar WRF 3.7.1 model (Hines and Bromwich 2008) was used to simulate meteorological conditions over Svalbard. The model was configured using polar projection with three one-way nested domains (Fig. 1). The outermost domain covers area around the Arctic Circle with spatial resolution of $27\text{ km} \times 27\text{ km}$

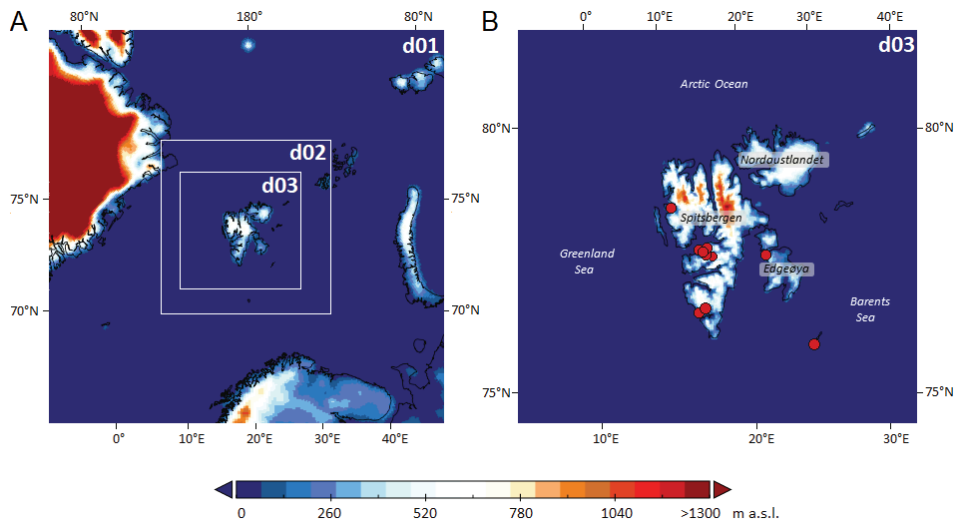


Fig. 1. Polar WRF domains used in this research. (A) three one-way nested domains (d01, d02 and d03); (B) innermost domain with location of measurement points over Svalbard.

(100×100 grid cells). To avoid rapid changes in the resolution between parent and nested domains, 1:3 ratio of downscaling was applied. The second nested domain has grid size of 9 km × 9 km (130×130 cells), and the innermost domain is focused on the Svalbard archipelago with 3 km × 3 km grid (277×277 cells). Vertically, all the domains use 48 sigma coordinated levels up to 50 hPa.

ERA-Interim reanalysis, available every 6 hours with spatial resolution of 0.75°×0.75° were used as initial and boundary conditions. Data were prepared using WRF Preprocessing System (WPS). The WPS USGS-based dataset for land use and land cover was used with resolution of 10 minutes for first (the outermost) domain and of 30 seconds for second and third inner domains (d02 and d03 on Fig. 1). Additionally, innermost domain (d03) includes high-resolution digital elevation model (DEM), developed by the Norwegian Polar Institute. Original high-resolution DEM was prepared as binary file, and interpolated to the final model mesh using WPS geogrid tool.

In this work, we analyze the results from the innermost domain and compare them with available in-situ measurements of air temperature and wind speed. The simulations were run for June 2008 and January 2009, with five days of spin-up time to account for the model to stabilize (Ulmer and Balss 2016). The baseline model configuration was similar to the one used by Bromwich *et al.* (2016), and use the Mellor-Yamada-Nakanishi-Niino Planetary Boundary Layer (PBL) scheme, the Goddard microphysics, the Kain-Fritsch *Cumulus* parameterization, and the RRTMG longwave and shortwave radiation schemes. Second, we have run the model 34 times, changing the baseline configuration in terms of long- and shortwave radiation, PBL and microphysics schemes. Additionally, we have calculated an ensemble mean (ENS) using all the model runs. The model runs are summarized in Table 1.

In our considerations, four groups of parameterization schemes were analyzed. First one refers to PBL schemes, where following ones were selected:

- **YSU** (The Yonsei University scheme; Hong *et al.* 2006): first-order closure nonlocal scheme, which establishes increased mixing at stable boundary layer, due to increasing the critical bulk Richardson number (from 0 to 0.25) (Hu *et al.* 2010).
- **MYJ** (The Mellor-Yamada-Janjic scheme; Janjic 1994): 1.5-order turbulence closure scheme. This scheme describes eddy diffusion coefficients from computing turbulent kinetic energy (TKE). Scheme is suitable for all stable and slightly unstable flows (Mellor and Yamada 1982).
- **MYNN 3** (The Mellor-Yamada-Nakanishi-Niino Level 3 scheme; Nakanishi and Niino 2009): second-order closure scheme, where expression of mixing length is adequate to a variety of static stability regimes. Stability is formulated in accordance with the results of large eddy diffusion (Cohen *et al.* 2015).

- **ACM2** (Asymmetric Convective Model version 2; Pleim 2007): first-order closure nonlocal scheme, where upward fluxes within the PBL are defined as the interaction between surface and separately each layers above (Cohen *et al.* 2015).

Table 1

Configurations of the WRF physics options used in this study. “BL0” means the baseline simulation as suggested by Bromwich *et al.* (2016). The scheme “RRTMG (F)”, corresponds to fast version of RRTMG (ra_sw_physics=24).

Simulation ID	Planetary Boundary Layer scheme	Microphysics scheme	Shortwave radiation scheme	Longwave radiation scheme
BL0	MYNN	Goddard	RRTMG	RRTMG
PBL1	YSU	Goddard	RRTMG	RRTMG
PBL2	MYJ	Goddard	RRTMG	RRTMG
PBL3	MYNN3	Goddard	RRTMG	RRTMG
PBL4	ACM2	Goddard	RRTMG	RRTMG
MP1	MYNN	Lin (Purdue)	RRTMG	RRTMG
MP2	MYNN	WSM 6	RRTMG	RRTMG
MP3	MYNN	Thompson	RRTMG	RRTMG
MP4	MYNN	WDM 6	RRTMG	RRTMG
SR1	MYNN	Goddard	Dudhia	RRTMG
SR2	MYNN	Goddard	Goddard	RRTMG
SR3	MYNN	Goddard	CAM	RRTMG
SR4	MYNN	Goddard	New Goddard	RRTMG
SR5	MYNN	Goddard	RRTMG (F)	RRTMG
LR1	MYNN	Goddard	RRTMG	RRTM
LR2	MYNN	Goddard	RRTMG	CAM
LR3	MYNN	Goddard	RRTMG	New Goddard

Second group of tested parameterizations refer to microphysics schemes (MP), where following were considered:

- **Lin (Purdue)**; 6-class scheme; Lin *et al.* 1983) refers to the following hydrometeors: water vapor, cloud ice, cloud droplets, snow, rain and graupel. Due to no interactions between horizontal grid points, this parameterization is convenient to massively parallel computation (Mielikainen *et al.* 2016).
- **WSM6** (WRF single-moment 6-class microphysics scheme; Hong and Lim 2006) developed on the base of WSM5 scheme (Hong *et al.* 2004), where graupel was added as another prognostic water substance variable.

- **WDM6** (WRF double-moment 6-class scheme; Lim and Hong 2010) includes the same prognostic variables as WSM6. Additionally, WDM6 adds predictive number concentration for cloud and rainwater with cloud condensation nuclei (CNN).
- **Thompson** (5-class scheme; Thompson *et al.* 2008) refers to the following hydrometeors: cloud water, cloud ice, rain, snow and graupel. Thompson scheme is single-moment, but for cloud ice variable becomes double-moment (the number concentration of cloud ice is also predicted).

The following shortwave radiation schemes (SR) were considered:

- **Dudhia** (Dudhia 1989): simple downward calculation; scheme includes integration of solar flux that accounts for clean-air scattering, water vapor absorption and cloud absorption, and reflection.
- **Goddard** (Chou and Suarez 1999; Chou *et al.* 2001): shortwave scheme which divides the solar spectrum into 11 spectral bands; interaction with resolved clouds.
- **New Goddard** (Chou and Suarez 1999): spectrum divided into 11 bands. This parameterization includes interactions with cloud fractions; scheme does not consider aerosols.
- **CAM** – NCAR Community Atmospheric Model (Collins *et al.* 2004): shortwave spectrum is divided into 19 bands. This parameterization has the ability to interact with cloud fractions, but additionally with aerosols and trace gases.
- **RRTMG** Rapid Radiative Transfer Model for GCMs (Iacono *et al.* 2008): scheme includes 14 shortwave bands with specified ozone profile and CO₂ and trace gases.

Three parameterizations describing longwave radiation (LR) were selected for using in model configuration:

- **RRTM** – The Rapid Radiative Transfer Model (Mlawer *et al.* 1997): spectral scheme developed using the correlated k-method, with specified ozone profile; includes interacts with resolved clouds.
- **CAM** – NCAR Community Atmospheric Model (Collins *et al.* 2004): 8 longwave bands; interactions with trace gases, aerosols and cloud fractions are included.
- **New Goddard** (Chou and Suarez 1999): 10 longwave bands; interactions with trace gases, aerosols and cloud fractions are included; ozone and CO₂ profiles are specified.

For further details, the reader is referred to the WRF mode user manual available on NCAR UCAR website (<http://www.mmm.ucar.edu>).

Evaluation of the model results. — The Polar WRF results from the innermost domain were compared with observational data from 10 stations situated over Svalbard (Fig. 1.). Spatial distribution of the measuring sites is uneven, with increased density in the center of the island, close to Longyearbyen. The stations are operated by Met Norway, the University of Svalbard (UNIS) and the Polish Academy of Sciences. The measurements were available for every hour, except for the Hopen Radio, where only 3-hourly interval was available. Further details related with stations' location used in this study are presented in Table 3. In this paper, simulated and observed air temperature and wind speed were analyzed. The domain-wide statistics (based on all the stations) have been calculated to summarize the model performance for each month and model run. For that, correlation coefficient (R) and standard deviation (SD) were calculated. Additionally, error statistics as mean error (ME) and mean absolute error (MAE) were used in model evaluation. Formulas of these statistics are similar, but in the case of ME (1), positive and negative values can be obtained, what give information about model over- and underestimating. Calculation of MAE (2) bases on absolute values, so only positive ones can be obtained. In the case of both ME and MAE the best expected value is 0.

$$ME = \frac{1}{N} \sum_{n=1}^N (sim_n - obs_n) \quad (1)$$

$$MAE = \frac{1}{N} \sum_{n=1}^N |sim_n - obs_n| \quad (2)$$

where:

sim – simulated value,

obs – observed value,

N – sample size.

The results were also analyzed spatially, to summarize the uncertainty of the model results, related to the selected parameterization schemes separately for PBL, MP, SR and LR. To do this, gridded monthly mean values (for air temperature and wind speed) were calculated for each model run within the PBL, MP, SR and LR group. Second, for each grid cell, standard deviation was calculated using monthly mean values from all simulations within each group. Because the standard deviation was calculated individually for each grid cell within the innermost domain, it was possible to present it in a map, showing

spatial changes of the model uncertainties, related to the selected parameterization. This was done to reveal the features of the model performance that could be related with selected options of physics and covered by simple comparison of the results with the sparse meteorological measurements clustered over the central Spitsbergen.

Table 3

Location details of meteorological stations.

Station name	Latitude (°N)	Longitude (°E)	Altitude (m a.s.l)	Data source
Adventdalen	78.198	15.838	15	UNIS
Breirosa	78.144	16.184	520	UNIS
Gruvefjellet	78.194	15.695	464	UNIS
Hansbreen	77.046	15.635	184	Polish Polar Station
Hopen Radio	76.510	25.013	6	Norwegian Meteorological Institute
Hornsund	77.002	15.536	10	Polish Polar Station
Kapp Lee	78.088	20.813	325	UNIS
Longyearbyen	15.567	78.217	448	Norwegian Meteorological Institute
Ny-Ålesund	78.917	11.933	12	Norwegian Meteorological Institute
Svalbard Lufthavn	78.245	15.502	28	Norwegian Meteorological Institute

Results

Meteorological conditions in June 2008 and January 2009. — To account for parameterization's sensitivity to possibly wide range of weather conditions on Svalbard, two months were selected as case studies: June 2008 and January 2009. Variability of meteorological elements during the investigated months for all stations (using box plots) is presented (Fig. 2).

Air temperatures for June 2008 were above 0°C for most of the time. Additionally temporal changes of this meteorological element were very low. In the beginning of January 2009, low temperature values at stations were recorded (usually below -15°C). Since the middle of the month, temperature

was increasing to values in range -8°C to 0°C . Based on boxes presented on Fig. 1, higher differences of measured temperature at stations can be observed on January 2009.

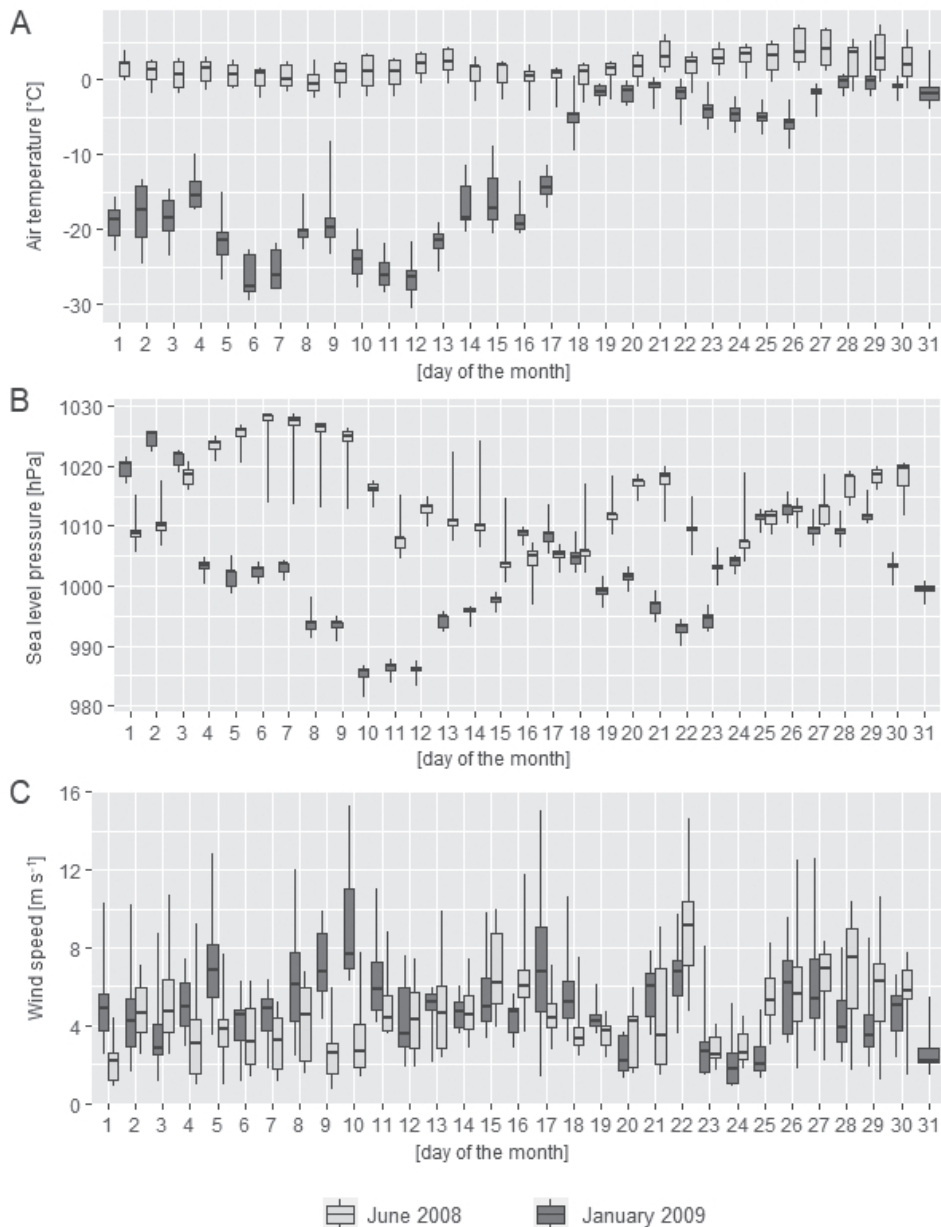


Fig. 2. Variability of selected meteorological elements during June 2008 and January 2009. (A) course of air temperature; (B) sea level pressure; (C) wind speed. Box plots present daily data from all considered stations.

At all considered stations, in June 2008 values of sea level pressure in range 997–1028 hPa were observed. Due to higher frequency of cyclones and atmospheric fronts in winter (Tsukernik *et al.* 2007), lower values of sea level pressure were present in January 2009 (with range of values 982–1027 hPa). Wind speed values are similar in two analyzed months. This meteorological element is characterized by the highest spatial variability. This can be an influence of numerous local effects mentioned earlier.

Evaluation of the Polar WRF model: statistical analysis. — Correlation coefficient values for simulated and observed air temperature is smaller in June 2008 (from 0.42 to 0.54) than in January 2009 (from 0.86 to 0.94; Fig. 3). This may be attributed to the lower temporal variability of air temperature observed in June, as presented in Fig. 2. In both months, negative values of ME show that the model underestimates the observed air temperature. Error statistics values (ME, MAE) are closer to 0 for January than for June. Values of ME range from -1.78°C to -6.03°C and MAE from 2.31°C to 6.71°C .

For June 2008, the impact of used PBL scheme can be observed if correlation coefficient is analyzed (Fig. 3). The simulation with the highest R is PBL2 and

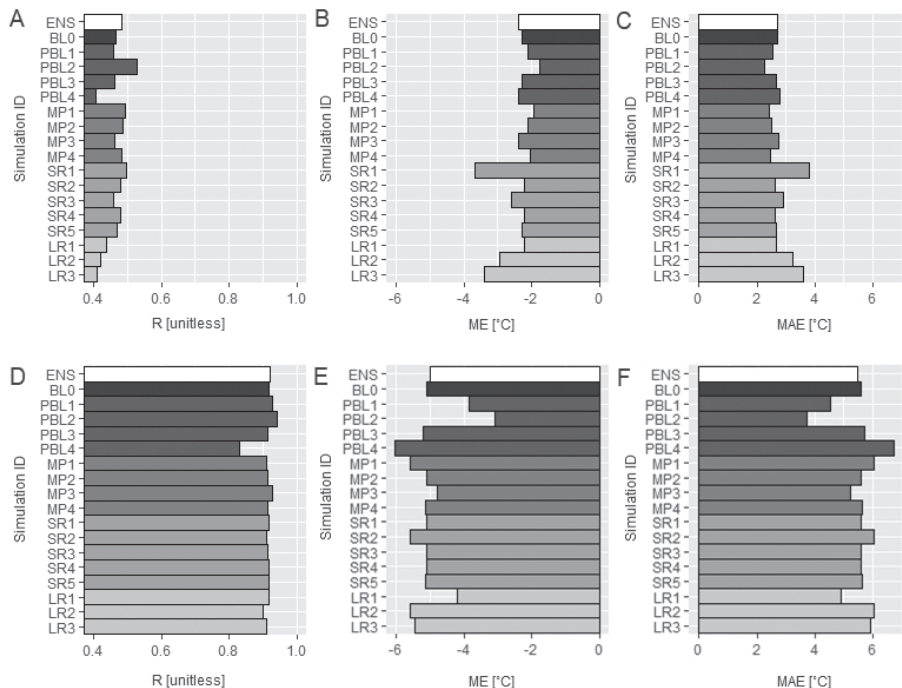


Fig. 3. Model performance for air temperature in two considered months; (A–C) statistic's values for June 2008; (D–F) model evaluation for January 2009. For each month correlation coefficient (A, D), mean error (B, E) and mean absolute error (C, F) were presented.

the lowest is PBL4, but the selection of MP, and especially SR or LR, has also large impact on the model results. ME and MAE values are the largest for SR1 simulation (respectively -3.70°C and 3.81°C), but are also relatively high for LR3.

Selection of the PBL scheme has the largest impact on the model performance also in January 2008. The lowest ME and MAE and the highest R are calculated for PBL2 model run, while the worst model performance is for PBL4. Selection of MP, SR or LR scheme has smaller impact on the model performance in January, and this is especially understandable for radiation during the polar night. In the case of ensemble average (ENS) in January 2009, ME and MAE values (respectively -5.02°C and 5.67°C) are higher than obtained for simulations PBL1, PBL2 and LR1. Ensemble mean does not improve the performance significantly.

Model errors for wind speed are summarized on Fig. 4. For June 2008, ME values show that the model may both over and underestimate the measurements, but the values are all within the $\pm 0.5 \text{ m s}^{-1}$. The largest ME values for June are calculated for PBL2 (0.27 m s^{-1}), but are similar, in terms of absolute value, also for LR1 (0.26 m s^{-1}), and LR3 (-0.30 m s^{-1}). It can be observed that ENS is characterized by the best result of MAE (2.72 m s^{-1}).

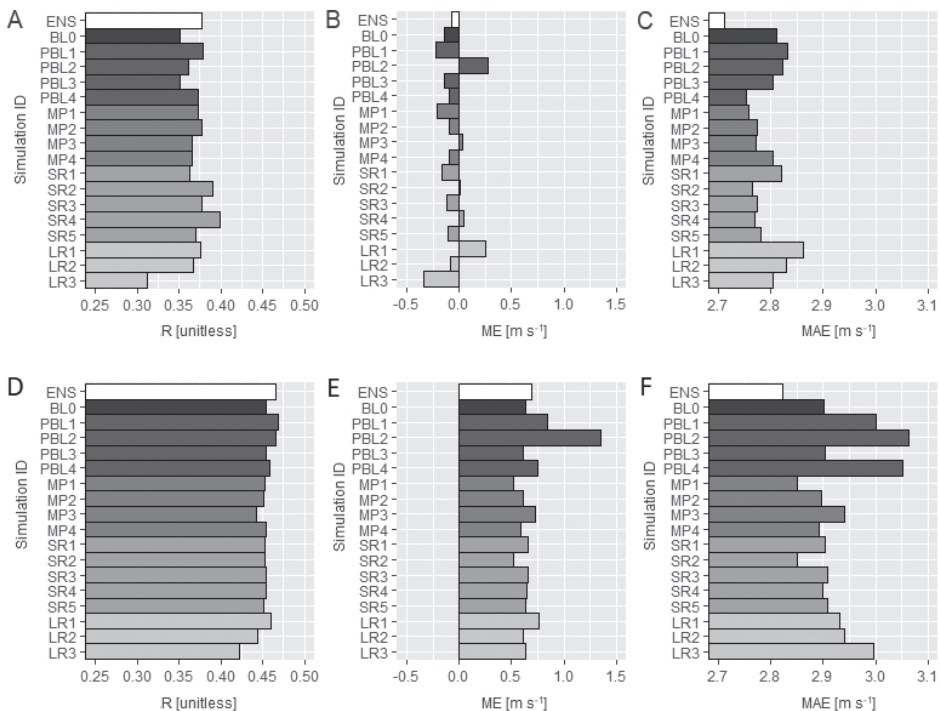


Fig. 4. Model performance for wind speed in two considered months; (A–C) statistic's values for June 2008; (D–F) model evaluation for January 2009. For each month correlation coefficient (A, D), mean error (B, E) and mean absolute error (C, F) were presented.

As for air temperature, the PBL scheme has very large impact on modeled wind speed, especially for January 2009, if ME and MAE are considered. Correlation coefficient does not change between the simulations except for LR3, which deteriorates the model performance in both January and June. ME and MAE are considerably higher for January if compared to June and are around 1.3 and 3.1 m s⁻¹, respectively, for ME and MAE. The highest ME and MAE are calculated for PBL2. According to MAE values, the best result was obtained for ENS (2.83 m s⁻¹).

Sensitivity of the parameterization schemes: spatial variability of simulations. — Because of the limited number of measurements and rather clustered location of the meteorological stations over the study area, we have made an attempt to further describe the differences between the model output by quantitatively comparing the maps of monthly mean air temperatures and wind speed. For each group of simulations (PBL, MP, LR and SR), standard deviation was calculated for each grid cell using data from all model runs within the group.

In June, spatial changes in SD are relatively small for all simulation groups. The obtained small range of its values (from 0 to 1.20°C) should be linked with fairly stable meteorological conditions in this month. In contrary to winter, the PBL (and MP) group shows relatively small spatial variability in SD during summer (Fig. 5). Spatial variability in SD is especially large for SR and LR schemes. For SR group, the largest SD values are observed over the land and over the sea areas in north eastern part of the model domain. For these areas, meteorological measurements are very limited, and simple comparison of model with measurements, presented above, may not reveal all these uncertainties. For LR group, the largest SD values are calculated for land areas. Increased SD for this group of model runs is also observed over the SE part of the model domain.

Much higher values of SD were obtained for January 2009, where maximum values are up to 3.70°C. For this month, obtained results are in agreement with the findings described by comparison of the model with the measurements (Fig. 6). Standard deviation between the model runs is the highest for the PBL group. Moreover, SD varies in space considerably for the PBL group. The highest values are calculated for the mountainous areas in the north of Svalbard, and are considerably lower in the south. This feature has not been revealed by comparison with meteorological measurements alone.

Spatial changes in SD for MP and SR runs are low and similar for both groups. Larger values are calculated for the coastal areas in the east of Spitsbergen. Very small SD values, close to zero, are for sea areas, especially the Greenland Sea. For LR runs, increased SD for air temperatures in January are observed over the northern areas of the model domain.

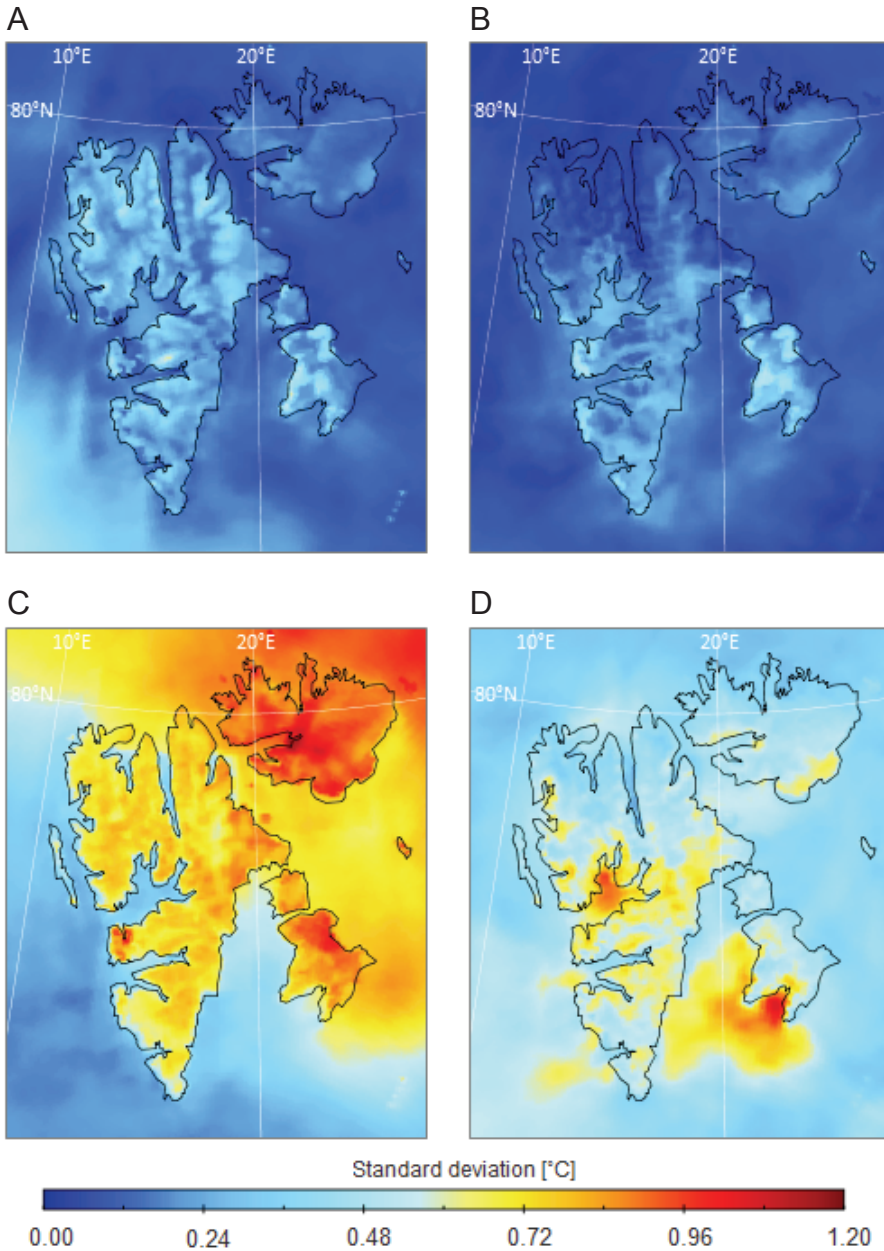


Fig. 5. Standard deviation of simulated mean monthly air temperature (°C) for each group of parameterization schemes in June 2008; (A) simulations with different PBL schemes; (B) MP schemes; (C) SR schemes; (D) LR schemes.

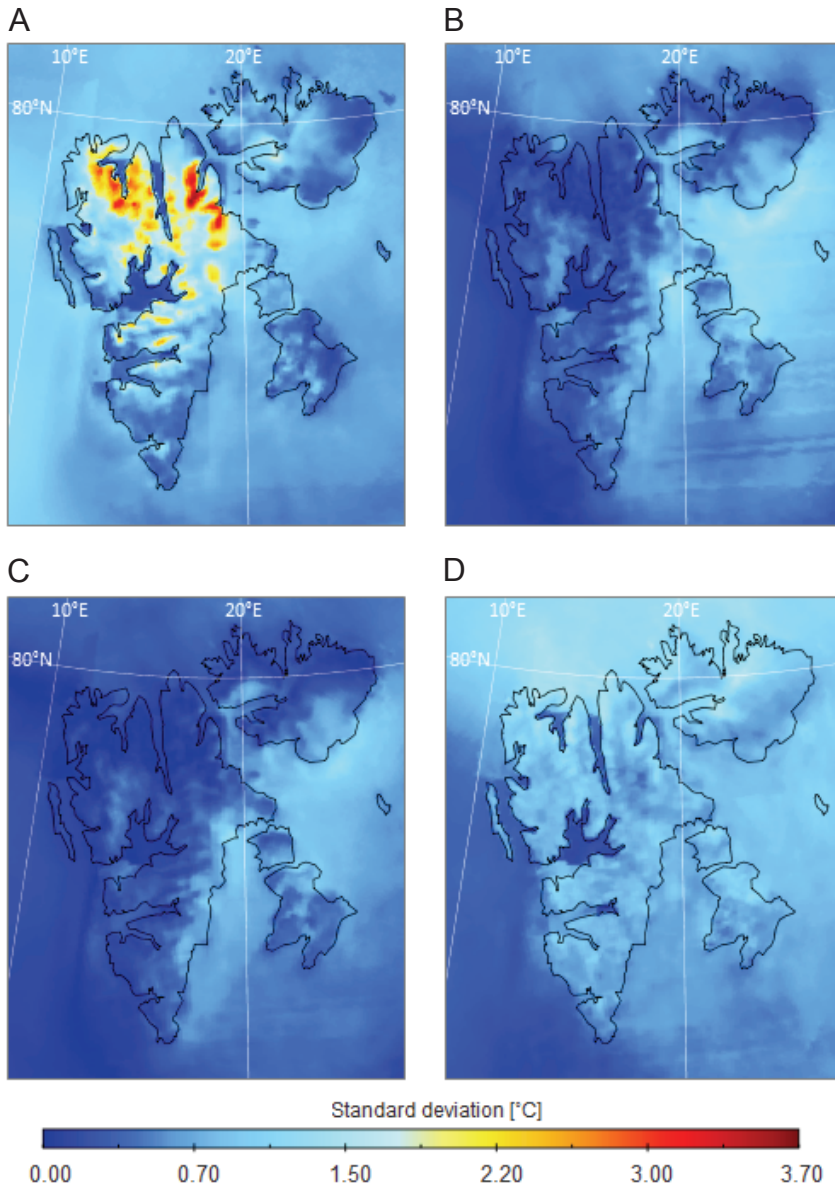


Fig. 6. Standard deviation of simulated mean monthly air temperature (°C) for each group of parameterization schemes in January 2009; (A) simulations with different PBL schemes; (B) MP schemes; (C) SR schemes; (D) LR schemes.

In analysis of wind speed, SD values do not exceed 0.7 m s^{-1} in June 2008 (Fig. 7). The largest variability between the model simulations, and the largest spatial changes of SD values, are calculated for PBL and SW groups. SD values are smaller for LR and especially MP group. There are noticeable

spatial differences between SD values for wind speed if all four groups of model runs are compared. For example, PBL group shows the highest values of SD along the eastern coast of Spitsbergen, while the largest values for SR are calculated for northern coast and for LR over the central land areas.

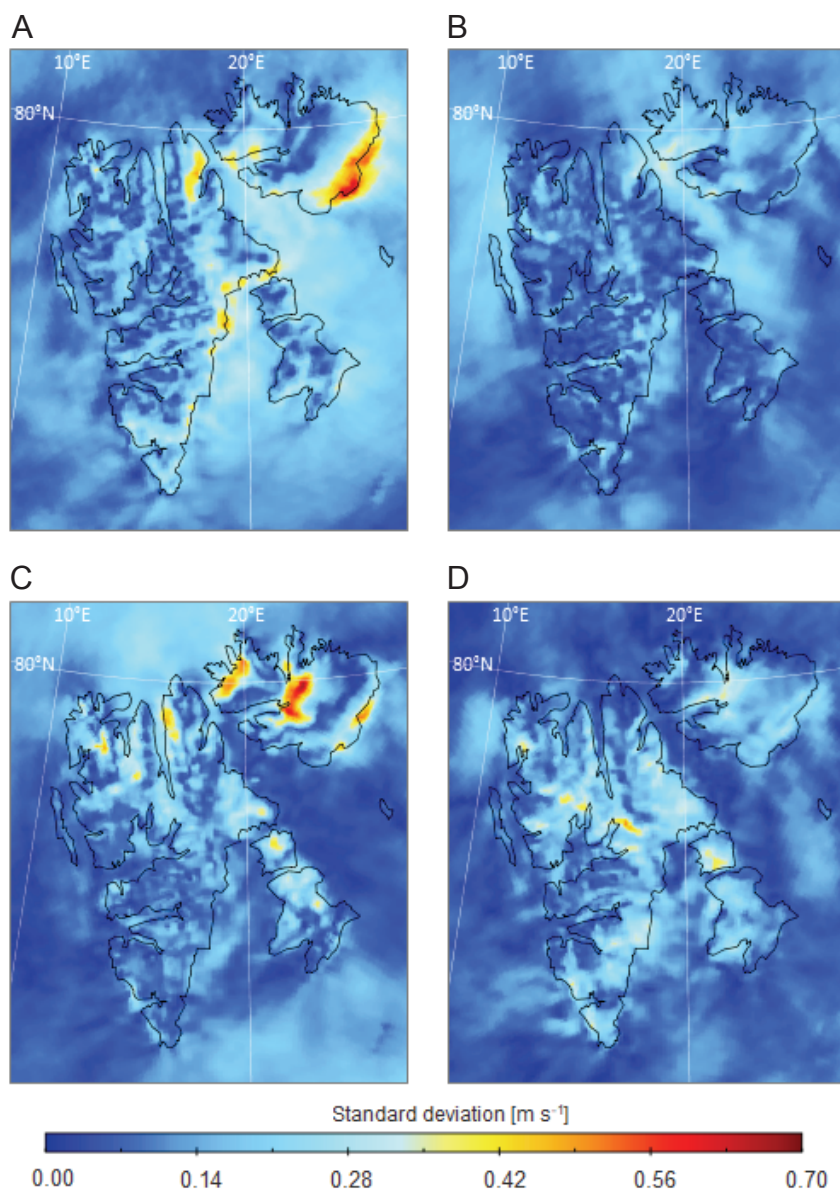


Fig. 7. Standard deviation of simulated mean monthly wind speed (m s⁻¹) for each group of parameterization schemes in June 2008; (A) simulations with different PBL schemes; (B) MP schemes; (C) SR schemes; (D) LR schemes.

In January 2009, SD values are slightly higher (up to 1.0 m s^{-1}). Similar to air temperature, SD values are the largest for the PBL group and over the land areas (Fig. 8), especially close to the coasts of southern Spitsbergen. SW group has very small SD over entire model domain. Both MP and LR groups show increased SD values close to the Nordaustlandet in NE part of the model domain.

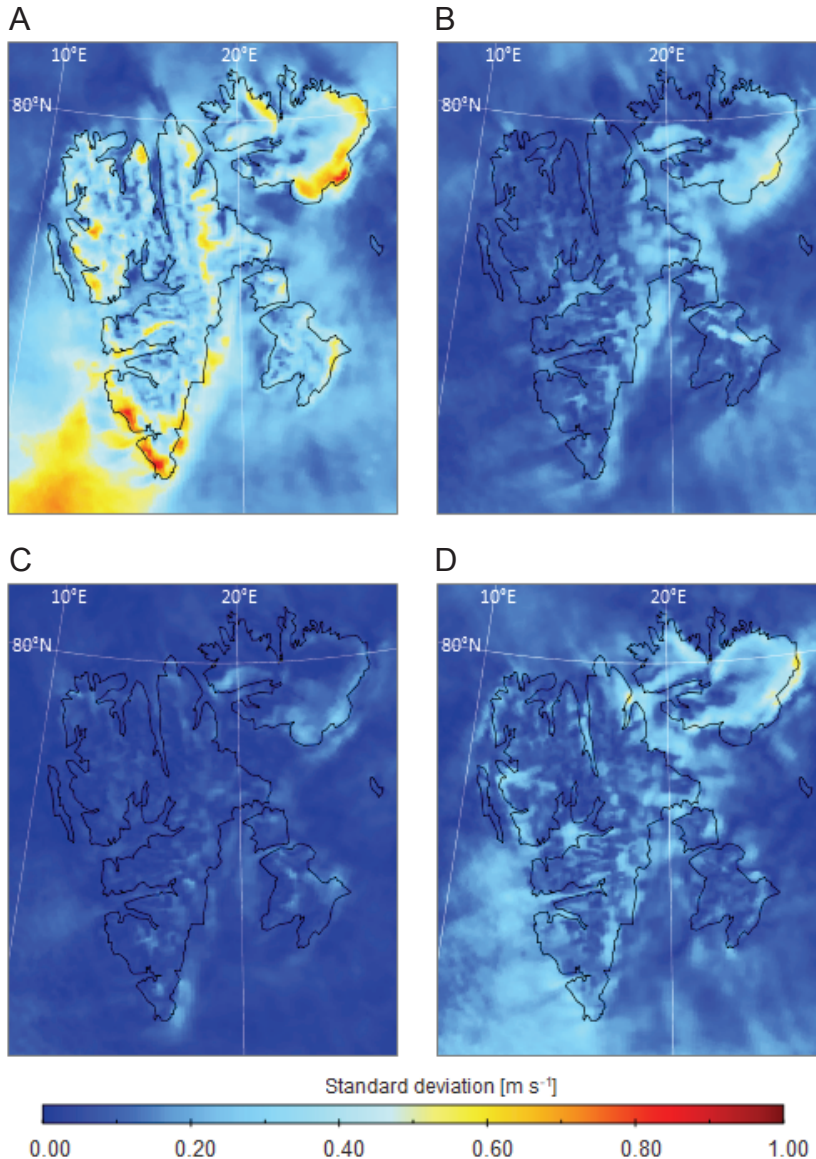


Fig. 8. Standard deviation of simulated mean monthly wind speed (m s^{-1}) for each group of parameterization schemes in January 2009; (A) simulations with different PBL schemes; (B) MP schemes; (C) SR schemes; (D) LR schemes.

Discussion

In this work, we have tested the role of the selected physical schemes on the results of the Polar WRF for air temperature and wind speed for two selected months. The analysis revealed that for the winter months (with January 2009 as an example), the selection of the planetary boundary layer scheme plays the largest role, both for air temperature and wind speed. The best model performance for air temperature was obtained for local scheme MYJ (PBL2), where the largest errors were typical for ACM2 scheme (PBL4), which uses local closure of air transport in vertical profile near the surface (Hu *et al.* 2010). For wind speed, simulation with MYNN3 scheme (PBL3) gave the smallest errors, and MYJ (which resulted in the closest agreement with measurements of air temperature) had the largest errors. The PBL schemes are characterized by different order of turbulence closure. Important are also assumptions about vertical mixing; some schemes are characterized by nonlocal closure, part of them by local ones. In the case of local closure schemes, turbulent fluxes are estimated at each grid point separately from gradients/mean values of atmospheric variables. This group of PBL schemes use prognostic turbulent kinetic energy (TKE) to determine eddy diffusion coefficients. Nonlocal schemes are often characterized by K-theory to define vertical mixing. There is a limitation of simulation turbulent mixing in neighbouring layers, so mixing can be incorrectly reproduced.

The local MYJ scheme has often been used as PBL scheme in model configuration in many Arctic and Antarctic applications of the WRF model (*e.g.* Wilson *et al.* 2011; Claremar *et al.* 2012; Bromwich *et al.* 2013). However, Claremar *et al.* (2012) have also shown that other PBL schemes, *e.g.* QNSE or MYNN2.5 performs better than MYJ, which also requires more computational resources. In wind speed and direction modeling provided by Láska *et al.* (2017) for fjords in Svalbard, QNSE scheme indicate slightly better results than YSU and MYJ. Noticeably, Bromwich *et al.* (2009) mentioned that selection of PBL or MP schemes has only small impact on the Polar WRF model performance. Our study confirms these findings only in terms of MP schemes, but also shows significant role of PBL schemes also for the areas not covered with measurement.

Results presented for January 2009 shows better agreement with measurements than for June 2008, if correlation coefficient is considered. However, for this month ME and MAE are also larger. Similar results were presented by Bromwich *et al.* (2009) for Arctic Ocean, with correlation coefficients close to 0.9 for January and air temperature. For wind speed, correlation coefficients presented by Bromwich *et al.* (2009) are significantly higher if compared with our study and exceed 0.78. This might be related with differences in model domain and configuration of the available measurements. In our study, the measuring sites are clustered in the central part of Svalbard, and most of the sites are located in Isfjorden.

There are very few studies that are focused on WRF model performance regarding the radiation schemes, and these studies are mostly focused on spring season (*e.g.* Kilpeläinen *et al.* 2011; Mäkiranta *et al.* 2011). Tastula and Vihma (2011) have tested RRTM, Dudhia and CAM schemes for Antarctic, concluding that these schemes do not affect the model performance significantly. Our results show that for the summer months the impact of the selected radiation scheme is significant and affect the model performance for air temperature and, to the smaller extent, wind speed. The highest errors were present in simulations using Dudhia shortwave radiation (SR1), New Goddard, CAM and RRTM longwave radiation schemes (LR1, LR2, LR3). These findings may also suggest that the application of the meteorological model integrated online with atmospheric chemistry model, that allows simulating the aerosol-radiation feedback mechanisms, might also be of large importance for these areas.

Ensemble mean values show rather limited added value for air temperature, but significantly improve the model agreement with measurements for wind speed in June 2008, especially in terms of MAE. This approach, which is based on simple averaging, shows the potential of the ensemble approach, but also the need for more careful selection of the ensemble members, as discussed *e.g.* by Solazzo *et al.* (2012).

Spatial analysis of the model results further reveals large model sensitivity especially to the PBL schemes, for both wind speed and air temperatures. Noticeably, the largest differences between the model runs are not necessarily calculated for the areas covered with meteorological measurements, and therefore suggest that the simple comparison of the model results with the measurements may be insufficient. Large variability among simulations was calculated for January 2009 over the northern part of Spitsbergen and over different fjords for the PBL schemes. Standard deviations for monthly average values were up to 3.5°C for air temperature and exceed 1 m s⁻¹ for wind speed over the southern part of Spitsbergen. This further supports the earlier mentioned conclusion on the importance of the PBL scheme for the WRF model result for Arctic. For June 2008, significant variability in air temperature is also observed for radiation schemes groups. In SR group, large standard variations are present over the whole land, but especially over northern part of Svalbard. Selection of LR scheme is important, especially near the largest fjord — Isfjorden, and western part of Edgeøya. Simulations inside mentioned groups of schemes (SR, LR) were not demonstrating significant differences between each other in spatial analysis of modeling results of wind speed, higher SD only for parts of Nordaustlandet.

Arctic is characterized by absence of typical diurnal radiation cycle, because of polar day and night phenomena. In effect, these circumstances cause a lack of diurnal cycle both of the basic meteorological values and of daily transformation of the PBL. Numerous investigations confirm that the arctic PBL is very shallow,

often not exceeding the depth of 200 m (Tjernström *et al.* 2004). PBL conditions and radiation budget are also modified by aerosol concentration. Its physical and chemical properties for fjords in Svalbard were investigated by Markuszewski *et al.* (2017) and Lisok *et al.* (2016). The aerosol-meteorology interactions were not included in our studies

Our study shows that the WRF model results for the Svalbard area are the most sensitive for selection of the PBL scheme. For January 2009, the smallest errors for air temperature were calculated for MYJ scheme, while the other model configuration options were the same as for Bromwich *et al.* (2016). For wind speed, the smallest errors are for MYNN3 scheme. For the summer month, the results are also strongly affected by selection of the radiation schemes. More studies are necessary to investigate other seasons.

Lack of meteorological measurements and uneven spatial distribution of meteorological stations in this area may influence the conclusions drawn from the analysis of the model error statistics. The spatial approach, where we compared the model runs for each group of simulations reveals some additional features. The role of each parameterization scheme changes spatially and in time. We have shown that there is large variability in the model results both for air temperature and wind speed if different PBL schemes are applied. This variability and its spatial changes are not fully revealed by comparing model results with the limited number of measurements.

Acknowledgements. — This work was supported by the National Science Centre (NCN), Poland (Grant No. UMO-2014/15/B/ST10/04455). The Polar WRF simulations were carried out in the Wrocław Centre for Networking and Supercomputing (<http://www.wcss.wroc.pl>), grant no 170. In this work, we have used the map data provided by the Norwegian Polar Institute. The authors would like to thank the anonymous reviewers for their constructive comments and suggestions to improve the quality of this paper.

References

- BROMWICH D.H., HINES K.M. and BAI L.S. 2009. Development and testing of polar weather research and forecasting model: 2. Arctic Ocean. *Journal of Geophysical Research* 114: doi:10.1029/2008JD010300.
- BROMWICH D.H., OTIENO F.O., HINES K.M., MANNING K.W. and SHILO E. 2013. Comprehensive evaluation of polar weather research and forecasting performance in the Antarctic. *Journal of Geophysical Research* 118: 274–292.
- BROMWICH D.H., WILSON A.B., BAI L.-S., MOORE G.W.K. and BAUER P. 2016. A comparison of the regional Arctic System reanalysis and the global ERA-Interim Reanalysis for the Arctic. *Quarterly Journal of the Royal Meteorological Society* 142: 644–658.
- CHOU M.-D. and SUAREZ M.J. 1999. *A solar radiation parameterization for atmospheric studies*. NASA Tech. Memo 104606, 15, 40 pp, National Aeronautics and Space Administration, Goddard Space Flight Center, Maryland, USA.

- CHOU M.D., SUAREZ M.J., LIANG X.Z., and YAN M.M.H. 2001. *A thermal infrared radiation parameterization for atmospheric studies*. NASA Tech Memo 104606, 19, 68 pp, National Aeronautics and Space Administration, Goddard Space Flight Center, Maryland, USA.
- CLAREMAR B., OBLEITNER F., REIJMER C., POHJOLA V., WACEGÅRD A., KARNER F. and RUTGERSSON A. 2012. Applying a mesoscale atmospheric model to Svalbard glaciers. *Advances in Meteorology* 2012: 321649.
- COHEN A.E., CAVALLO S.M., CONGILIO M.C. and BROOKS H.E. 2015. A review of planetary boundary layer parameterization schemes and their sensitivity in simulating southeastern U.S. cold season severe weather environments. *Weather and Forecasting* 30: 591–612.
- COLLINS W.D., RASCH P.J., BOVILLE B.A., HACK J.J., MCCAA J.R., WILLIAMSON D.L., KIEHL J.T. and BRIEGLEB B. 2004. Description of the NCAR Community Atmosphere Model (CAM 3.0). *NCAR Technical Note*: NCAR/TN-464+STR.
- CZERNECKI B. and PÓLROLNICZAK M. 2013. Initial assessment of the weather research and forecasting model for forecasting bioclimatic conditions during breeze circulation – case study of the Słowiński National Park. *Quaestiones Geographicae* 32: doi: 10.2478/quageo-2013-0021.
- DUDHIA J. 1989. Numerical study of convection observed during the Winter Monsoon Experiment using a mesoscale two-dimensional model. *Journal of Atmospheric Science* 46: 3077–3107.
- GIORGI F. and GUTOWSKI JR W.J. 2015. Regional dynamical downscaling and the CORDEX initiative. *Annual Review of Environment and Resources* 40: 467–490.
- HEIKKILÄ U., SANDVIK A. and SORTEBERG A. 2011. Dynamical downscaling of ERA-40 in complex terrain using the WRF regional climate model. *Climate Dynamics* 37: 1551–1564.
- HINES K.M. and BROMWICH D.H. 2008. Development and testing of Polar WRF. Part I. Greenland ice sheet meteorology. *Monthly Weather Review* 136: 1971–1989.
- HINES K.M., BROMWICH D.H., BAI L.-S., BARLAGE M. and SLATER A.G. 2011. Development and testing of Polar WRF. Part III. Arctic land. *Journal of Climate* 24: 26–48.
- HODKINSON I.D., WEBB N.R., BALE J.S., BLOCK W., COULSON S.J. and STRATHDEE A.T. 1998. Global change and Arctic ecosystems: conclusions and predictions from experiments with terrestrial invertebrates on Spitsbergen. *Arctic and Alpine Research* 30: 306–313.
- HONG S.-Y., DUDHIA J. and CHEN S.-H. 2004. A revised approach to ice microphysical processes for the bulk parameterization of clouds and precipitation. *Monthly Weather Review* 132: 103–120.
- HONG S.-Y. and LIM J.-O. 2006. The WRF single-moment 6-class microphysics scheme (WSM6). *Journal of the Korean Meteorological Society* 42: 129–151.
- HONG S.-Y., NOH Y. and DUDHIA J. 2006. A new vertical diffusion package with an explicit treatment of entrainment processes. *Monthly Weather Review* 134: 2318–2341.
- HONG S.-Y. and KANAMITSU M. 2014. Dynamical downscaling: fundamental issues from an NWP point of view and recommendations. *Asia-Pacific Journal of Atmospheric Sciences* 50: 83–104.
- HU X.-M., NIELSEN-GAMMON J.W. and ZHANG F. 2010. Evaluation of three boundary layer schemes in the WRF model. *American Meteorological Society* 49: 1831–1844.
- IACONO M.I., DELAMERE J.S., MLLAWER E.J., SHEPHARD M.W., CLOUGH S.A. and COLLINS W.D. 2008. Radiative forcing by long-lived greenhouse gases: calculations with the AER radiative transfer models. *Journal of Geophysical Research* 113: doi:10.1029/2008JD009944.
- JANJIC Z.I. 1994. The step-mountain eta coordinate model: further developments of the convection, viscous sublayer, and turbulence closure schemes. *Monthly Weather Review* 122: 927–945.
- KILPELÄINEN T., VIHMA T., MANNINEN M., SJÖBLOM A., JAKOBSON E., PALO T. and MATURILLI M. 2012. Modelling the vertical structure of the atmospheric boundary layer over Arctic fjords in Svalbard. *Quarterly Journal of the Royal Meteorological Society* 138: 1867–1883.
- KILPELÄINEN T., VIHMA T. and ÓLAFSSON H. 2011. Modelling of spatial variability and topographic effects over Arctic fjords in Svalbard. *Tellus* 63A: 223–237.

- KOTLARSKI S., KEULER K., CHRISTENSEN O.B., COLETTE A., DÉQUÉ M., GOBIET A., GOERGEN K., JACOB D., LÜTHI D., VAN MEIJGAARD E., NIKULIN G., SCHÄR C., TEICHMANN C., VAUTARD R., WARRACH-SAGI K. and WULFMEYER V. 2014. Regional climate modeling on European scales: a joint standard evaluation of the EURO-CORDEX RCM ensemble. *Geoscientific Model Development* 7: 1297–1333.
- KUMAR A., BHOWMIK S.K.R. and DAS A.K. 2012. Implementation of Polar WRF for short range prediction of weather over Maitri region in Antarctica. *Journal of Earth System Science* 121: 1125–1143.
- LÁSKA K., CHLÁDOVÁ Z. and HOŠEK J. 2017. High-resolution numerical simulation of summer wind field comparing WRF boundary-layer parametrizations over complex Arctic topography: case study from central Spitsbergen. *Meteorologische Zeitschrift* 26: 4: 391–408.
- LAW K.S. and STOHL A. 2007. Arctic air pollution: origins and impacts. *Science* 315: 1537–1540.
- LIM K.-S.S. and HONG S.-Y. 2010. Development of an effective double-moment cloud microphysics scheme with prognostic cloud condensation nuclei (CCN) for weather and climate models. *Monthly Weather Review* 138: 1587–1612.
- LIN Y.-L., FARLEY R.D. and ORVILLE H.D. 1983. Bulk parameterization of the Snow field in a cloud model. *American Meteorological Society* 22: 1065–1092.
- LISOK J., MARKOWICZ K.M., RITTER C., MAKUCH P., PETELSKI T., CHILINSKI M., KAMINSKI J.W., BECAGLI S., TRAVERSI R., USISTI R., ROZWADOWSKA A., JEFIMOW M., MARKUSZEWSKI P., NEUBER R., PAKSZYS P., STACHLEWSKA I.S., STRUZEWSKA J., ZIELINSKI T. 2016. 2014 iAREA campaign on aerosol in Spitsbergen – Part 1: Study of physical and chemical properties. *Atmospheric Environment* 140: 150–166.
- MARKUSZEWSKI P., ROZWADOWSKA A., CISEK M., MAKUCH P., PETELSKI T. 2017. Aerosol physical properties in Spitsbergen’s fjords: Hornsund and Kongsfjord during AREX campaigns in 2014 and 2015. *Oceanologia* 59: 460–472.
- MÄKIRANTA E., VIHMA T., SJÖBLOM A. and TASTULA E.-M. 2011. Observations and modelling of the atmospheric boundary layer over sea-ice in a Svalbard fjord. *Boundary-Layer Meteorology* 140: doi:10.1007/s10546-011-9609-1.
- MELLOR G.L. and YAMADA T. 1982. Development of a turbulence closure model for geophysical fluid problems. *Reviews of Geophysics and Space Physics* 20: 851–887.
- MIELIKAINEN J., HUANG B. and HUANG H.-L.A. 2016. Optimizing Purdue-Lin microphysics scheme for Intel Xeon Phi Coprocessor. *IEEE Journal of Selected Topics in Applied Earth Observations and Remote Sensing* 9: 425–438.
- M LAW E.J., TAUBMAN S.J., BROWN P.D., IACONO M.J. and CLOUGH S.A. 1997. Radiative transfer for inhomogeneous atmospheres: RRTM, a validated correlated-k model for the longwave. *Journal of Geophysical Research* 102: 16663–16682.
- NAKANISHI M. and NIINO H. 2009. Development of an improved turbulence closure model for the atmospheric boundary layer. *Journal of the Meteorological Society of Japan* 87: 895–912.
- PLEIM J.E. 2007. A combined local and nonlocal closure model for the atmospheric boundary layer. Part II: application and evaluation in a mesoscale meteorological model. *Journal of Applied Meteorology and Climatology* 46: 1396–1409.
- RADIĆ V., BLISS A., BEEDLOW A.C., HOCK R., MILES E. and COGLEY J.G. 2014. Regional and global projections of twenty-first century glacier mass changes in response to climate scenarios from global climate models. *Climate Dynamics* 42: 37–58.
- ROTHROCK D.A., YU Y. and MAYKUT G.A. 1999. Thinning of the Arctic Sea-Ice cover. *Geophysical Research Letters* 26: 3469–3472.
- SKAMAROCK W.C., KLEMP J.B., DUDHIA J., GILL D.O., BARKER D.M., WANG W. and POWERS J.G. 2005. *A description of the advanced research WRF version 2*. NCAR Technical Note NCAR/TN-468STR: 88 pp, National Center for Atmospheric Research, Boulder, Colorado, USA.

- SOLAZZO E., BIANCONI R., VAUTARD R., APPEL K.W., MORAN M.D., HOGREFE C., BESSAGNET B., BRANDT J., CHRISTENSEN J.H., CHEMEL C., COLL I., VAN DER GON H.D., FERREIRA J., FORKEL R., FRANCIS X.V., GRELL G., GROSSI P., HANSEN A.B., JERICEVIC A., KRALJEVIC L., MIRANDA A.I., NOPMONGCOL U., PIROVANO G., PRANK M., RICCIO A., SARTELET K.N., SCHAAP M., SILVER J.D., SOKHI R.S., VIRA J., WERHAHN J., WOLKE R., YARWOOD G., ZHANG J., RAO S.T. and GALMARINI S. 2012. Model evaluation and ensemble modelling of surface-level ozone in Europe and North America in the context of AQMEII. *Atmospheric Environment* 53: 60–74.
- STEMPNIEWICZ L., BŁACHOWIAK-SAMOŁYK K. and WĘSŁAWSKI J.M. 2007. Impact of climate change on zooplankton communities, seabird populations and Arctic terrestrial ecosystem—A scenario. *Deep Sea Research Part II: Topical Studies in Oceanography* 54: 2934–2945.
- STROEVE J., HOLLAND M.M., MEIER W., SCAMBOS T. and SERREZE M. 2007. Arctic sea ice decline: faster than forecast. *Geophysical Research Letters* 34: L09501.
- TASTULA E.-M. and VIHMA T. 2011. WRF Model Experiments on the Antarctic Atmosphere in Winter. *American Meteorological Society* 139: 1279–1291.
- THOMPSON G., FIELD P.R., RAMUSSEN R.M. and HALL W.D. 2008. Explicit forecasts of winter precipitation using an improved bulk microphysics scheme. Part II: Implementation of a new snow parameterization. *Monthly Weather Review* 136: 5095–5115.
- TJERNSTRÖM M., LECK C., PERSSON P.O.G., JENSEN M.L., ONCLEY S.P. and TARGINO A. 2004. The summertime Arctic atmosphere meteorological measurements during the Arctic Ocean Experiment 2001. *Bulletin of American Meteorological Society*, doi:10.1175/BAMS-85-9-1305.
- TSUKERNIK M., KINDIG D.N. and SERREZE M.C. 2007. Characteristics of winter cyclone activity in the northern North Atlantic: insights from observations and regional modeling. *Journal of Geophysical Research* 112: D03101.
- ULMER F.G. and BALSS U. 2016. Spin-up time research on the weather research and forecasting model for atmospheric delay mitigations of electromagnetic waves. *Journal of Applied Remote Sensing* 10: 016027.
- VIHMA T., PIRAZZINI R., FER I., RENFREW I.A., SEDLAR J., TJERNSTRÖM M., LÜPKES C., NYGÅRD T., NOTZ D., WEISS J., MARSAN D., CHENG B., BIRNBAUM G., GERLAND S., CHECHIN D. and GAFSCARD J.C. 2014. Advances in understanding and parameterization of small-scale physical processes in the marine Arctic climate system: a review. *Atmospheric Chemistry and Physics* 14: 9406–9450.
- WASSMANN P., DUARTE C.M., AGUSTI S. and SEJR M.K. 2011. Footprints of climate change in the Arctic marine ecosystem. *Global Change Biology* 17: 1235–1249.
- WILSON A.B., BROMWICH D.H. and HINES K.M. 2011. Evaluation of Polar WRF forecasts on the Arctic system reanalysis domain: Surface and upper air analysis. *Journal of Geophysical Research* 116: D11112.

Received 5 March 2018

Accepted 9 July 2018